https://doi.org/10.5194/egusphere-2026-2611
Preprint. Discussion started: 30 June 2026

Thermo-hydrological and thermo-mechanical modeling of freezing soil and frost quake occurrence

Jarkko Okkonen[2], Christian B. Silbermann[4], Jere Remes[1], Dmitri Naumov[4,6], Nikita Afonin[3], Elena Kozlovskaya[3], Emma-Riikka Kokko[3], Kari Moisio[3], Tymofiy Gerasimov[5], and Thomas Nagel[4,6,7]

[1]Geological Survey of Finland, P.O. Box 96, FI-02151 Espoo, Finland
[2]Geological Survey of Finland, P.O. Box 97, FI-67101 Kokkola, Finland
[3]Oulu Mining School, Faculty of Technology, P.O. Box 3000, FI-90014, University of Oulu
[4]Technische Universität Bergakademie Freiberg, Geotechnical Institute, Gustav-Zeuner-Str. 1, 09599 Freiberg, Germany
[5]BGE Technology GmbH, Eschenstraße 55, 31224 Peine, Germany
[6]Helmholtz Centre for Environmental Research GmbH (UFZ), Department of Environmental Informatics, Permoserstr. 15, 04318 Leipzig, Germany
[7]Technische Universität Bergakademie Freiberg, Freiberg Centre for Water Research (ZeWaF), 09599 Freiberg, Germany

Correspondence to: Jarkko Okkonen (jarkko.okkonen@gtk.fi)

Abstract. Frost quakes are seismic events originating in frozen ground, traditionally attributed to ice expansion when air temperature decreases rapidly, the soil is saturated and has little or no snow cover. However, novel observations presented here question the necessity of some of the previous assumption and meteorological conditions, driving us to consider alternative mechanisms. This study investigates frost quake formation through numerical modeling and seismological and hydrological observations in Tähtelä, Finland, during winter 2022–2023. We analyzed soil and atmospheric conditions during frost quake occurrences, noting a strong correlation with rapid air temperature decrease below -20°C, and with varying snow cover. We modeled the thermo-hydrological (TH) processes, such as cryosuction-driven ice lens growth, using Amanzi-ATS, while the thermo-mechanical (TM) evolution was modeled with OpenGeoSys (OGS). The ATS TH simulation results suggest an important role of cryosuction for the appearance of frost quakes. Focusing on volumetric effects, the OGS TM simulation results reveal tensional and shear stress rates in the soil, both of which are able to cause fracturing leading to frost quakes. Future work should integrate fully-coupled thermo-hydro-mechanical simulations and laboratory experiments to refine predictive models and assess infrastructure risks in cold climates.

1 Introduction

The arctic and sub-arctic regions are warming two to four times faster than other regions on the planet (Rantanen et al., 2022), which has consequences for the hydrological cycle, especially in winter. Changes in wintertime hydrological processes, such as the amount of rain and snow and their interrelation, the variability of snow cover and snow melt, the freezing and thawing of soil, the depth of frozen soil and the soil water content, affect the Earth's Critical Zone (CZ) – the interface that connects vegetation, surface and subsurface layers, and groundwater (Brantley et al., 2007). These changes will have a direct impact on the ecosystems in the CZ, such as wetlands and forests, but also on urban infrastructure, including roads and built environment

https://doi.org/10.5194/egusphere-2026-2611
Preprint. Discussion started: 30 June 2026

(Brantley et al., 2007; Giardino and Houser, 2015; Parsekian et al., 2015; Laine, 2016; Sipola, 2024). Understanding the dynamic processes within the CZ in response to changing weather conditions is crucial to assessing the resilience of both natural and built environments.

One notable consequence of a warming climate in the arctic and sub-arctic regions is the acceleration of the hydrological cycle, increasing the frequency and intensity of extreme events (IPCC, 2023). These events contribute to structural damage in both landscapes and infrastructure, often manifesting itself as fractures caused by variations in precipitation, snow melt, and freeze-thaw cycles. In freezing/thawing soil such fractures may develop suddenly with the release of seismic energy, known as *frost quakes*, or through slower, aseismic processes such as *frost heave*. Frost quakes have been observed in rural areas in several countries, recently fairly prominently, e. g., in Finland (Afonin et al., 2024; Okkonen et al., 2020; Laine, 2016; Sipola, 2024), and in Canada (Battaglia and Changnon, 2016; Leung et al., 2017). Frost quakes can be detected by national seismic networks (Okkonen et al., 2020; Afonin and Kozlovskaya, 2019), or by local instrumentation (e. g. Afonin et al., 2024; Goto et al., 1980) measuring their origin and magnitude as well as ground acceleration and velocity. Frost quakes usually originate in the upper layers of the soil and can produce loud noise or structural vibrations. For example, Afonin et al. (2024) detected and located 17 frost quakes in soil in the Tähtelä area and 17 ice quakes[1] in the River Kitinen on 6.1.2023 during an abrupt drop in air temperature. Those originating in soils produced ground accelerations large enough to be able to damage infrastructure (Afonin et al., 2024).

The prevailing explanation for frost quakes, as summarized by Battaglia and Changnon (2016), is that they occur due to saturated soil expanding during a sudden drop in temperature. Their review outlines the key meteorological conditions commonly associated with frost quake occurrence:

1. rapid saturation from thaw, rain, or flooding to increase soil water content,
2. minimal or no snow cover to limit insulation effects,
3. rapid decline of sub-freezing temperatures.

However, in the absence of on-site data on frost quakes, no detailed mechanistic modeling studies have been conducted to verify the proposed causes behind frost quakes yet. In this article we analyze the novel observational data that complicates the common narrative on the meteorological conditions necessary for frost quakes to occur, which serves as a compelling reason to re-assess the mechanism behind the phenomenon.

In an effort to gain a more complete mechanical understanding of the situation, we need to work towards a fully-integrated thermo-hydro-mechanical consideration which takes into account all of the potential stressors and their interplay. This naturally includes the consideration of the growth of ice lenses, but also e. g. the contraction of cooling ice. This is due to the following reasoning: if the soil temperature is initially sub-freezing at shallow depths relevant for the phenomenon, much of the water in the pores is already frozen and would contract as the temperature decreases. Snowmelt being negligible at consistently sub-freezing conditions, a significant increase of the frozen layer would require either an influx of liquid water via cryosuction

[1] An *ice quake* is attributed to large ice bodies, where seismic events are caused by a sudden cracking of ice.

https://doi.org/10.5194/egusphere-2026-2611
Preprint. Discussion started: 30 June 2026

or the expansion of the residual unfrozen water exceeding the thermal contraction of ice and soil matrix. This presents two competing mechanisms: the contraction of rapidly cooling ice versus the growth of ice lenses (by either the addition of liquid water by cryosuction or by the freezing of the *in situ* residual water), both of which could plausibly contribute to stress buildup and crack formation under different conditions.

There is precedence for both arguments. The frost heave due to cryosuction-driven growth of ice lenses is well understood, as we will discuss later. Meanwhile, thermal contraction fractures have been associated with ice quakes – cryoseisms originating in ice rather than soil (Lombardi et al., 2019) – as well as ice floe cracking (Evans and Untersteiner, 1971). Additionally, we should note Kavanaugh et al. (2019), who proposed a "jacking" mechanism, where initial contraction-induced cracks fill with liquid water, which then freezes and expands, triggering an ice quake. These studies along with the theoretical considerations highlight that the role of thermal contraction in frost quakes cannot be dismissed off-hand without detailed research.

Gilpin (1980) developed a model for ice lens formation and growth based on the Clapeyron equation, which describes the relationship between pressure and temperature while accounting for the latent heat of fusion. Originally applied in soil science to study capillary pressure in nonfreezing conditions, the Clapeyron equation has since been extended to freezing soils to explain cryosuction-driven ice lens growth (Derjaguin and Churaev, 1978). A more recent model of ice lens formation by Style et al. (2011) assumes that an initial ice lens fills a flaw in the soil, leading to crack propagation when the pressure exerted by the growing ice exceeds the material's critical stress intensity factor K_{Ic} (fracture toughness). The crack continues to grow until it reaches a material boundary.

Recent studies have explored how ice growth contributes to stress accumulation in confined environments. Gerber et al. (2022, 2023); Style et al. (2023) examined stress buildup around ice under controlled temperature gradients. Gerber et al. (2022) demonstrated experimentally that under these conditions, water migrates to undercooled regions, causing stress to increase until ice growth is constrained by confining forces. Localized stress accumulation increases the likelihood of ice-induced damage. Style et al. (2023) further analyzed the pressure buildup in confined systems, deriving a linear Clapeyron equation for the water-ice equilibrium. Their findings show that volumetric expansion of ice in confined conditions can generate pressures of nearly $11\ \mathrm{MPa}$ per Kelvin of undercooling when residual liquid water remains. This cryosuction-driven stress, where undercooled ice extracts water from its surroundings and exerts pressure on pore walls, is a major driver of frost-induced damage in sub-arctic and arctic regions. Gerber et al. (2023) experimentally investigated cryosuction and ice pressure in polycrystalline ice, showing that polycrystallinity accelerates stress buildup in freezing wet porous media, increasing its damage potential. Schollick et al. (2016) studied the formation of ice lenses by freezing of a dispersion of colloidal silica particles in water. They found that a larger temperature gradient caused ice lenses to be initiated more frequently. Moreover the variations of particle packing density affected the lens thickness and consequently the amount and rate of heave.

Other thermo-hydro-mechanical simulation studies of freeze-thaw cycles in soils include Aukenthaler et al. (2016); Haxaire et al. (2017); Korshunov et al. (2020); Tuohino et al. (2021). These studies employed the proprietary finite element analysis software Plaxis to model the impact of the freeze-thaw cycle on e. g. road surfaces. However, to our knowledge, no comprehensive thermo-hydro-mechanical models specifically addressing frost quakes have been developed.

https://doi.org/10.5194/egusphere-2026-2611
Preprint. Discussion started: 30 June 2026

A recent study by Okkonen et al. (2020) attempted to quantify crack development associated with frost quakes by modeling thermally-induced stresses as a function of temperature changes and soil properties. These stresses are then compared to the critical stress intensity factor (K_{Ic}) of the pre-cracked materials to assess fracture propagation (Okkonen et al., 2020). However, this approach does not account for subsurface processes such as cryosuction-driven ice lens growth, which locally increases capillary pressure and contributes to stress buildup in the surrounding soil (Peppin and Style, 2013; Style et al., 2011). Although these mechanisms influence fracture development, a detailed understanding of their role remains challenging due to assumptions of isotropy in the modeling framework.

In this study, we are striving towards a deeper understanding of frost quakes by the application of two different modeling approaches:

1. TH: thermo-hydrological modeling of a partially saturated soil column including capillary and cryosuction effects;
2. TM: thermo-mechanical modeling of a fully-saturated soil column including thermal and phase-change volume strains.

The separation of these physical mechanisms is meant to identify correlations and causal relations to frost quakes.[2]

In Section 2, we review the study site in Tähtelä and summarize the seismological observations conducted there. A soil station was installed to monitor soil water content and temperature at various depths, which are used to calibrate the coupled models introduced later. Subsurface water content and temperature measurements began in October 2022, and frost quakes were recorded during the winter of 2022–2023. We briefly provide some common theoretical preliminaries from thermodynamics and the theory of porous media, which we will always refer to in the subsequent sections. We use the thermo-hydrological model, Amanzi-ATS (Coon et al., 2020), to simulate snow accumulation, soil temperature, soil water, ice and gas content and cryosuction in Tähtelä, and compare results with dates of frost quakes. We outline the theory of cryosuction pressure, soil water, ice and gas content in the TH model. Model parametrization, calibration and observation of soil temperature and soil water content are briefly discussed. We use the thermo-mechanical model, OpenGeoSys (OGS) (Zheng et al., 2022, 2017; Bilke et al., 2019), to explore stresses in soil attributed to freezing and describe the TM theory of soil freezing and associated stresses. We also explain the one-way coupling between ATS and OGS models.

In Section 3 we present both the observational results and the simulation results, i. e. cryosuction induced by ice growth from Amanzi-ATS and cryostresses obtained from OGS, based on thermal and freezing volume strains. We also examine how these results correlate with observed frost quake incidents. Finally, Section 5 provides a broader discussion of the findings and future venues for further research.

2 Materials and methods

2.1 Study site and local seismological observations during extreme winter weather events 2022–2023

The study site is located in northern Finland in the city of Sodankylä (67.37°N, 26.63°E), in an area called Tähtelä, which is also the location of the Sodankylä geophysical observatory (Fig. 1a). The area is characterized by arctic climate condi-

[2]Of course, in reality all these effects occur at the same time making a holistic understanding and modeling extremely difficult.

https://doi.org/10.5194/egusphere-2026-2611
Preprint. Discussion started: 30 June 2026

tions, with the average winter temperature being around -10°C and snow depth reaching up to 90 cm and beyond (https://en.ilmatieteenlaitos.fi/download-observations, last access: November 2024). The deep and predominantly sandy soil is unconsolidated. Field observations also confirmed that the soil was homogeneous at all depths.

We established a soil station in October 2022 to monitor soil temperature and water content (CS615, Campbell Scientific, Logan, UT, USA) at depths of 10 cm, 20 cm, 30 cm, 50 cm, 80 cm. Soil samples were collected from the installation site. One sample was taken at a depth of 10 cm and another at 50 cm. A third sample was taken from the pile that was dug out, i. e. constituting a mixed soil sample. Particle size distributions were determined with sieve analysis. From the samples, d_{10} and d_{60} were determined and the Kozeny-Carman method (Odong, 2007) was used to estimate permeability.

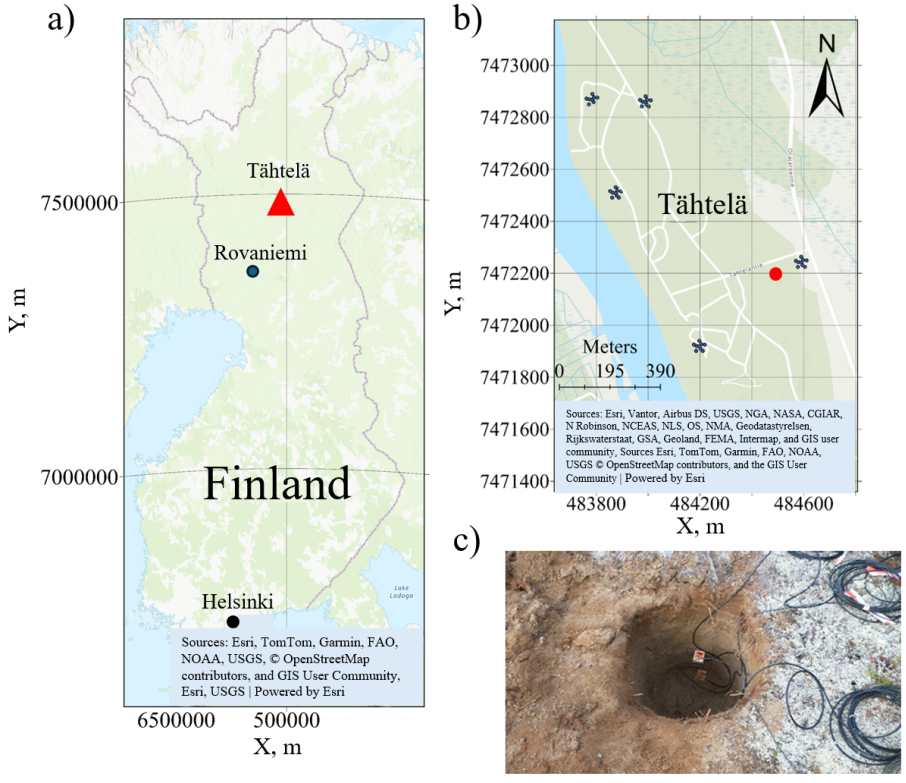

Figure 1. (a) Study site location; (b) soil station and seismic array locations. The red dot shows the soil station, the green dots indicate the arrays of short-period seismic stations; (c) soil station installation. The coordinate system is EUREF_FIN_TM35FIN (units are in meters; X is easting and Y is northing).

For the seismological observation of frost quakes, a total of 45 seismic instruments in five seismic arrays were installed in Tähtelä (Fig. 1b). Each of the arrays consisted of nine short-period three-component seismic stations equipped with GSB autonomous data recorders and GS-One LF geophones by Geospace Technologies Ltd. (USA). Configurations of the arrays were selected using recommendations by Schweitzer et al. (2012). These arrays recorded continuous seismic data from October

https://doi.org/10.5194/egusphere-2026-2611
Preprint. Discussion started: 30 June 2026

130 2022 to the end of May 2023 with a sampling frequency of 500 Hz. To detect and localize frost quakes, data was prefiltered by a bandpass filter of 2–20 Hz and seismic records were stacked for each of the arrays using a beamforming algorithm (Schweitzer et al., 2012). Next, P and S wave arrivals were manually picked from the stacked seismograms and coordinates were calculated and origin times determined using a seismic velocity model of the soils (Afonin et al., 2024).

The frost quakes most often originate during extreme winter weather events, like abrupt temperature change (Okkonen 135 et al., 2020; Afonin et al., 2024), and thus the results of seismological observations during such events in the Tähtelä during winter 2022-2023 were analyzed. The locations of frost quakes originating in soils are shown in Fig. 2: These frost quakes are presented in different colors depending on the day of occurrence. There are two clear clusters of frost quake locations. The first cluster is located in a wetland area near the river. The second cluster is on the area of Sodankylä geophysical observatory.

From November 2022 to January 2023, most seismicity was observed in the wetland in the NE and irrigated channels in the 140 SW. This seismicity could be related thin snow coverage of the ground during these months that was unable to protect ground from abrupt freezing.

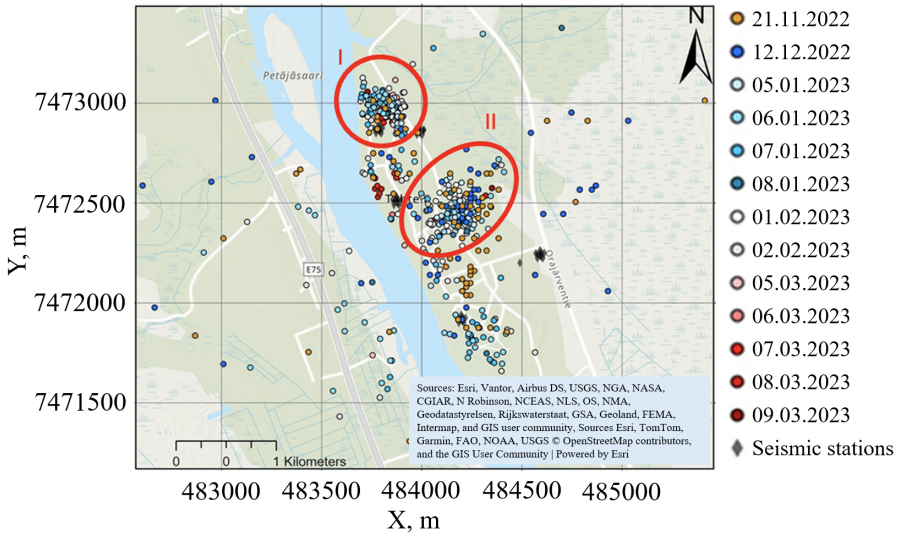

Figure 2. Sources of frost quake events originating in soils during winter 2022–2023. Capital I marks the first cluster of events while capital II marks the second cluster.

2.2 Theoretical preliminaries

The models used in the following share the common features of a multi-phasic continuum approach for porous media: each phase is associated with a volume fraction (also called phase content). Assuming the pore space (porosity ϕ) to be filled with 145 the phases ice (I), water (W) and gas (G) gives

$$\phi_{\mathrm{I}} + \phi_{\mathrm{W}} + \phi_{\mathrm{G}} = \phi \,, \tag{1}$$

https://doi.org/10.5194/egusphere-2026-2611
Preprint. Discussion started: 30 June 2026

with the remaining solid phase $\phi_S = 1 - \phi$. Division by porosity yields corresponding saturations fulfilling the condition

$$S_I + S_W + S_G = 1 \, . \tag{2}$$

In contrast to the partial densities, the phases' real (R) mass densities are denoted as $\varrho_{IR}, \varrho_{WR}, \varrho_{SR}$. Further, T denotes the thermodynamic temperature and p the (phase) pressure. More specifically, p_I, p_W and p_G are ice, water and gas pressure, respectively. $T_m = 273.15$ K is used as the melting/fusion temperature of ice. The enthalpy $L > 0$ required to melt a substance is called specific latent heat of melting/fusion. More specifically, L_m is the specific latent heat of melting ice at the bulk temperature T_m. Further, for each phase λ denotes the thermal conductivity, c_p is the isobaric specific heat capacity, and α_T the linear thermal expansivity. In this paper, only 2D (quasi 1D) problems are studied, where a cartesian base system is used with coordinates x, y and time t. Balance equations for energy, mass and momentum are completed by constitutive equations. The resulting transient coupled multi-field problems are solved by numerical first-order implicit time-stepping schemes.

2.2.1 Thermo-hydrological modeling of freezing soil

This Section aims to test the hypothesis that ice lens growth driven by cryosuction is the dominant mechanism behind frost quakes. To this end, thermo-hydrological modeling of a partially saturated soil column is used.

We applied the Advanced Terrestrial Simulator (ATS v. 1.3) (Coon et al. (2020)) to simulate snow accumulation and melt, soil water, ice and gas content, soil temperature and capillary pressure at different depths. ATS uses the mimetic finite difference method for solving hydrological and thermal problems (Coon et al., 2020). In this study, it was used to simulate the hydrological cycle, including water flow, energy transport, as well as snow accumulation and melt in both surface and subsurface environments. It has been successfully applied to permafrost modeling (Sjöberg et al., 2016; Gao and Coon, 2022). The subsurface model describes liquid water, ice, and gas interactions using a Richards-type mass balance equation, incorporating Darcy's law for flow dynamics. The surface model includes overland flow based on a diffusion wave approximation and an energy balance equation that accounts for surface water freezing. These systems are coupled by demanding the continuity of pressure, temperature, and flux conditions, with surface equations acting as boundary conditions for the subsurface model (Coon et al., 2020).

2.2.2 Cryosuction and ice content

As mentioned above, a main mechanism behind frost heave is the growth of ice lenses, and a similar model is necessary to be considered for frost quakes, too. Experimentally it is well-known that once ice has formed in soil, it has the potential of sucking liquid water leading to the growth of ice lenses. Since there is only a small supply of water available at any single location, the growth of ice lenses requires a suction to supply liquid water. Thus cryosuction and ice lens pressure are linked. Cryosuction can be modeled with the Clapeyron equation, which connects pressure and temperature via phase change enthalpy. The Clapeyron equation in a soil system at temperature T is of the form

$$p_I - p_W = \rho_{WR} L_m \theta, \quad \text{with} \quad \theta = \frac{T - T_m}{T_m} \, , \tag{3}$$

https://doi.org/10.5194/egusphere-2026-2611
Preprint. Discussion started: 30 June 2026

where the shifted dimensionless temperature θ was introduced. As the specific latent heat of fusion is positive ($L_\mathrm{f} > 0$ means heat must be supplied for melting), the pressure difference $p_\mathrm{I} - p_\mathrm{W}$ is negative in the cryoregime $\theta < 0$. Consequently, it is a cryosuction indeed. In the following text, $p_\mathrm{I} - p_\mathrm{W}$ is called cryosuction.[3] Assuming a homogeneous material and an isotropic mechanical state, the pore ice pressure p_I can be used as a proxy for the mechanical stress.

Based on the Clapeyron equation and a van Genuchten model (van Genuchten, 1980) used to relate suction to the unfrozen water content, Painter and Karra (2014) proposed a constitutive model to calculate ice saturation S_I and water saturation S_W in soils:

$$S_\mathrm{W} = \begin{cases} S_\mathrm{vG}\left((p_\mathrm{W} - p_\mathrm{I})\beta\right), & \theta < \theta_\mathrm{f}, \\ S_\mathrm{vG}\left((p_\mathrm{G} - p_\mathrm{W})\right), & \theta \geq \theta_\mathrm{f}, \end{cases} \quad \text{with} \quad \theta_\mathrm{f} = \frac{\Psi_\mathrm{vG}(1 - S_\mathrm{G})}{\beta L_\mathrm{f} \rho_\mathrm{W}}, \tag{4}$$

$$S_\mathrm{I} = 1 - \frac{S_\mathrm{W}}{S_\mathrm{vG}(p_\mathrm{G} - p_\mathrm{W})}, \tag{5}$$

where β is the ratio of ice–water to water–air surface tensions for non-colloidal soils. $S_\mathrm{vG}(\Delta p)$ is a functional relationship between some saturation S and some pressure difference Δp given by the van Genuchten model under unfrozen conditions, and Ψ_vG is its inverse function (Painter and Karra, 2014).[4] Equation (4) has been used in the multi-field simulator Amanzi-ATS (Coon et al., 2020) as well as in a field-scale application for a permafrost site (Gao and Coon, 2022). The function S_vG is given by Painter and Karra (2014):

$$S_\mathrm{vG}(\Delta p) = S_\mathrm{r} + (1 - S_\mathrm{r})\left[1 + (\alpha \Delta p)^n\right]^{-m}, \tag{6}$$

where S_r is the residual saturation, m and $n = \frac{1}{1-m}$ are dimensionless exponents and α is a scaling parameter with the unit Pa^{-1} (inverse of the so-called bubble pressure). Recapitulating the model equations from above it now becomes clear that the cryosuction follows the soil temperature in a nonlinear way.

2.2.3 ATS model domain and simulation parameters

The simulated column domain (Figure 3) measured $1\ \mathrm{m} \times 1\ \mathrm{m} \times 25\ \mathrm{m}$ containing 182 cells.The vertical grid resolution varied to capture critical processes: 2 cm spacing from the surface to the depth of 2.2 m, and then we gradually increased grid spacing from 5 cm to 50 cm to the bottom of the domain at 25 m. We initially started from 5 cm grid spacing from the top surface to 2.2 m and gradually decrease the cell size from 5 cm 2 cm to estimate the model response to cell size. Bigger cells size (5 cm) did not cause any numerical instabilities nor affected computational times but had some effect on soil water and ice content and soil temperature. For example at the depth of 30 cm mean soil water content and ice content with 2 cm grid spacing were 0.081 [-], 0.42 [-] and with 5 cm grid spacing they were 0.079 [-] and 0.044 [-] and the maximum soil water and ice content with 2 cm grid spacing were 0.148 [-] and 0.101 [-] and with 5 cm grid spacing they were 0.148 [-] and 0.106 [-]. The minimum, maximum and mean soil temperatures with 2 cm grid spacing were $-2.14°\mathrm{C}$, $20.77°\mathrm{C}$ and $4.16°\mathrm{C}$ and with 5 cm grid spacing

[3] From the view of soil physics, it constitutes an energy density with the meaning of a suction potential.

[4] As the argument of the van Genuchten function usually is a *capillary* pressure, it is tempting to call the pressure difference $p_\mathrm{I} - p_\mathrm{W}$ likewise. However, from the physical point of view, only the pressure difference $p_\mathrm{G} - p_\mathrm{W}$ gives rise to capillary effects.

https://doi.org/10.5194/egusphere-2026-2611
Preprint. Discussion started: 30 June 2026

they were $-1.96°\mathrm{C}$, $20.55°\mathrm{C}$ and $4.15°\mathrm{C}$. Thus 2 cm cell size was chosen to fully capture the highly dynamic soil water and ice content and soil temperature dynamics at the topsoil. The gradual increase of cell size from 2.2 m to bottom of model domain was chosen to avoid any numerical issues of increasing cell size too fast. In Amanzi-ATS solution is limited to a maximum saturation of water and ice, and time is integrated using the adaptive time stepping scheme. In this study, maximum time step is 3600 seconds and maximum change in water and ice saturation in a time step is 0.1 [-]. The groundwater table, averaging 5 m below the surface (Marttila et al., 2021), was represented using a constant head boundary condition at this depth. The aquifer is unconfined, with minimal seasonal fluctuations in groundwater level (Marttila et al., 2021). Simulations were performed with 1 hour time step.

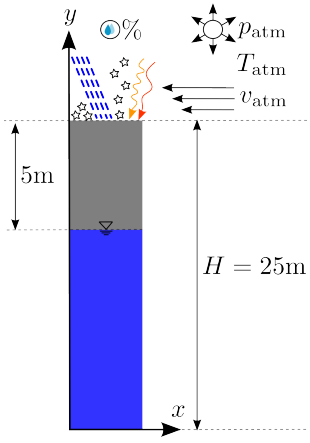

Figure 3. Sketch of the ATS simulation domain with boundary conditions. Pictograms represent incoming short and long wave radiation, precipitation rain and snow as snow water equivalent, as well as atmospheric wind speed, humidity, pressure and temperature, all of which are functions of time. The data in Tähtelä was sourced from the Finnish Meterorological Institute Open Data, Weather Observations

Hydraulic properties were assigned based on grain size distribution analysis: the permeability was set to $3.83 \cdot 10^{-11}$ m^2 based on $d_{10} = 0.137$ mm and $d_{60} = 0.275$ mm. The best fit between simulated and observed soil water content and temperature was achieved with van Genuchten parameters $\alpha = 0.03576\ \mathrm{Pa}^{-1}$ and $m = 0.1754$ for Equation (6). The thermal conductivity of Tähtelä aligns with similar unconsolidated sandy soil found in central Finland (Arola et al., 2016). The parameters of unfrozen (wet) and dry soil are 2.69 $\mathrm{W\,m^{-1}\,K^{-1}}$ and 0.15 $\mathrm{W\,m^{-1}\,K^{-1}}$, respectively. The effective thermal conductivity of the bulk material includes air, soil, water and ice contributions (Coon et al., 2020). Table 1 provides remaining parameters.

λ_{S} [$\mathrm{W\,m^{-1}\,K^{-1}}$]	$c_{p\mathrm{S}}$ [$\mathrm{J\,kg^{-1}\,K^{-1}}$]	α_T^{S} [$\mathrm{K^{-1}}$]	ϕ [-]
2.69*	840*	2625*	0.3

Table 1. Soil parameters from on-site measurements, applied both for OGS and ATS simulation runs (Arola et al., 2016)*.
λ_{SR} is the soil's thermal conductivity, $c_{p\mathrm{S}}$ is the soil's specific heat capacity, ϕ is the porosity of the porous solid matrix.
The material parameters for all phases are summarized in Table A1.

https://doi.org/10.5194/egusphere-2026-2611
Preprint. Discussion started: 30 June 2026

2.3 Thermo-mechanical modeling of freezing soil

Alternatively to the hypothesis that ice lens growth driven by cryosuction is the dominant mechanism behind frost quakes, volumetric thermal and phase change strains could be significant. In order to test this hypothesis, thermo-mechanical modeling of a fully-saturated soil column is performed. This allows for a separate consideration of the straining effects.

2.3.1 Model concept: OpenGeoSys (OGS)

Here we apply the open-source multi-field finite element simulator OpenGeoSys (OGS) (Kolditz et al., 2012; Bilke et al., 2019; Naumov et al., 2024). In the fully-coupled thermo-mechanical process, OGS takes into account latent heat and volumetric expansion of freezing water. In contrast to the Amanzi ATS model (cf. previous section), fully water-saturated conditions are assumed while the water phase remains hydraulically implicit in the model (i. e. there is no water pressure present, no water flow in the transport equations and no hydro-mechanical coupling).[5] OGS does not account for snow accumulation and melt. Therefore, we extract and use 1 hour soil surface temperature from ATS as boundary condition in OGS. The initial soil temperature profile calculated by ATS is also imported as initial condition into OGS.

2.3.2 Thermo-mechanics of a freezing-thawing soil

For thermo-mechanical modeling we assume the following simplifications:

- purely elastic mechanical behavior (no plastic compaction),
- linear thermal expansion,
- fully saturated pore space (no gas phase).

Full saturation implies in the context of freezing $\phi_\mathrm{I} + \phi_\mathrm{W} = \phi$. The corresponding saturations fulfill the condition $S_\mathrm{I} + S_\mathrm{W} = 1$, with S_I representing the saturation of the pore space with ice. To quantify the amount of pore ice, a phase-change indicator function $S_\mathrm{I}(T)$ is introduced such that $\phi_\mathrm{I} := \phi S_\mathrm{I}(T)$. A Heaviside-like function of temperature T is used here, which takes a value of 1 indicating ice if T drops below the freezing temperature T_m, and equals 0 otherwise (liquid water). In the numerical computations, a regularized (smoothed) counterpart of the above step-wise function is used, i. e.

$$S_\mathrm{I}(T) := \frac{1}{1 + e^{k(T - T_\mathrm{m})}}, \quad k > 0. \tag{7}$$

The energy balance equation with phase change (and without external heat sources) for some physical domain Ω reads:

$$\left((\varrho c_p)^\mathrm{eff} - \varrho_\mathrm{IR} L_\mathrm{m} \frac{\mathrm{d}\phi_\mathrm{I}}{\mathrm{d}T} \right) (T)'_\mathrm{S} - \boldsymbol{\nabla} \cdot \left(\lambda^\mathrm{eff} \cdot \boldsymbol{\nabla} T \right) = 0 \quad \text{in } \Omega, \tag{8}$$

[5] Likewise, the solid phase remained mechanically implicit in the ATS model.

https://doi.org/10.5194/egusphere-2026-2611
Preprint. Discussion started: 30 June 2026

where $(T)'_{\mathrm{S}}$ is the temperature's material time derivative following the solid motion and $\boldsymbol{\nabla}$ is the Nabla vector operator. The effective (mixture) properties, i. e. the heat capacity and the thermal conductivity, are given by

$$(\varrho c_p)^{\mathrm{eff}} = (1-\phi)\varrho_{\mathrm{SR}} c_{p\mathrm{S}} + (\phi - \phi_{\mathrm{I}})\varrho_{\mathrm{WR}} c_{p\mathrm{W}} + \phi_{\mathrm{I}}\varrho_{\mathrm{IR}} c_{p\mathrm{I}},$$
$$\lambda^{\mathrm{eff}} = (1-\phi)\lambda_{\mathrm{SR}} + (\phi - \phi_{\mathrm{I}})\lambda_{\mathrm{WR}} + \phi_{\mathrm{I}}\lambda_{\mathrm{IR}}.$$

Note that we only consider isotropic heat conduction in the model. However, since the ice saturation and volume fraction depend on the temperature field $T(t,x,y)$, the effective (mixture) properties are space-dependent, too. Within the linear elasticity assumptions, the standard thermo-elastic stress-strain relation for a deformable, fully-saturated porous medium in which the pore water can change its phase (freezing–thawing) reads as follows (Bluhm et al., 2011):

$$\boldsymbol{\sigma}(\boldsymbol{\varepsilon}_{\mathrm{S}}, \boldsymbol{\varepsilon}_{\mathrm{I}}, T) = \mathbb{C}_{\mathrm{S}} : \left[\boldsymbol{\varepsilon}_{\mathrm{S}} - \alpha_T^{\mathrm{S}}(T - T_{\mathrm{S}0})\mathbf{I}\right] + \phi_{\mathrm{I}}\mathbb{C}_{\mathrm{I}} : \left[\boldsymbol{\varepsilon}_{\mathrm{I}} - \alpha_T^{\mathrm{I}}(T - T_{\mathrm{I}0})\mathbf{I} - \alpha_{\phi_{\mathrm{I}}}(S_{\mathrm{I}}(T) - S_{\mathrm{I}0})\mathbf{I}\right]. \tag{9}$$

Here, the first term describes the deformation of a solid matrix (skeleton), whereas the second term accounts for the deformation of the ice. The stress contributions for both solid matrix and ice are almost identical: The isotropic fourth-order elasticity tensors for the solid matrix and the ice phase differ only by the elastic constants, i. e. $\mathbb{C}_{\mathrm{S}} = \mathbb{C}(E_{\mathrm{S}}, \nu_{\mathrm{S}}), \mathbb{C}_{\mathrm{I}} = \mathbb{C}(E_{\mathrm{I}}, \nu_{\mathrm{I}})$. The corresponding strains are $\boldsymbol{\varepsilon}_{\mathrm{S}}$ and $\boldsymbol{\varepsilon}_{\mathrm{I}}$. Linear thermal expansion coefficients are defined as α_T^{S} and α_T^{I}. The additional term present in the ice phase strain accounts for the 9 % volumetric expansion occurring during water freezing, with $\alpha_{\phi_{\mathrm{I}}}$ being the corresponding parameter.[6] Quantities with the index zero indicate reference values typically given by initial conditions.

Kinematically, following Bluhm et al. (2011), a specific relation between the strain tensors $\boldsymbol{\varepsilon}_{\mathrm{S}}$ and $\boldsymbol{\varepsilon}_{\mathrm{I}}$ is adopted. It is based on the assumption that the motions of ice and solid are *identical* except for an initial solid motion, that is $\boldsymbol{\varepsilon}_{\mathrm{S}} = \boldsymbol{\varepsilon}_{\mathrm{S}0} + \boldsymbol{\varepsilon}_{\mathrm{I}}$, where $\boldsymbol{\varepsilon}_{\mathrm{S}0}$ represents the strain accrued by the solid matrix before the onset of the water-to-ice phase transition (Bluhm et al., 2011).

2.4 OGS model domain and simulation parameters

The OGS 1D model domain (Figure 4) is similar to that of the ATS model domain (Figure 3), with a depth of 25 m. We mechanically confined the domain on all sides but on the top (to allow for frost heave) and used homogeneous Neumann boundary conditions to thermally isolate the sides while setting constant temperature on the bottom and time-dependent temperature on the top (Figure 4). The bottom boundary was fixed at 5°C. Temperature on top of the model domain (i. e. soil surface) was imported from the ATS simulations. This one-way coupling allowed us to study soil freezing and mechanical behavior beneath the snow cover. The domain was meshed with quad elements using linear shape functions, and the parameters are listed in Table 1. The time step for the simulations was 1 hour (as in the ATS simulations).

[6] While in the TH model from ATS, the ice phase takes effect by a temperature-dependent cryosuction, in the TM model from OGS the phase change water–ice induces volumetric strains.

https://doi.org/10.5194/egusphere-2026-2611
Preprint. Discussion started: 30 June 2026

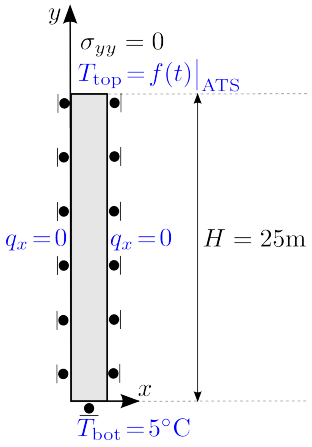

Figure 4. Sketch of the OGS simulation domain with mechanical and thermal boundary conditions.

3 Results

We conducted multiple ATS simulations with different parameter combinations and compared the results to observed soil water content and temperature. Here, we present the best-fit results, with parameter values given in Section 2.2.3 and Appendix A. In the simulations we used 1 hour time step but daily values are presented. Field observations confirmed that the soil was homogeneous at all depths, allowing for non-layered modeling. For the OGS simulations, we used the same soil parameters as in ATS (Table 1).

3.1 Observable soil parameters and thermo-hydraulic simulation results

Figure 5a) shows the observed air temperature as a time series, while Figure 5b) presents the observed and ATS-simulated snow depths. Air temperature reaching $-20°$C closely coincided with frost quake occurrences under sub-zero soil conditions (Figure 8e). During the winter 2022–2023, snow accumulation began on 21.10.2022 and thawing ended by 17.5.2023. Simulated and observed snow accumulation and melt fit well together, with ATS capturing the variation in snow cover as well. During the later frost quake observations between 7.–9.3.2023 the observed snow cover was 78 cm and the simulated one was 73 cm.

https://doi.org/10.5194/egusphere-2026-2611
Preprint. Discussion started: 30 June 2026

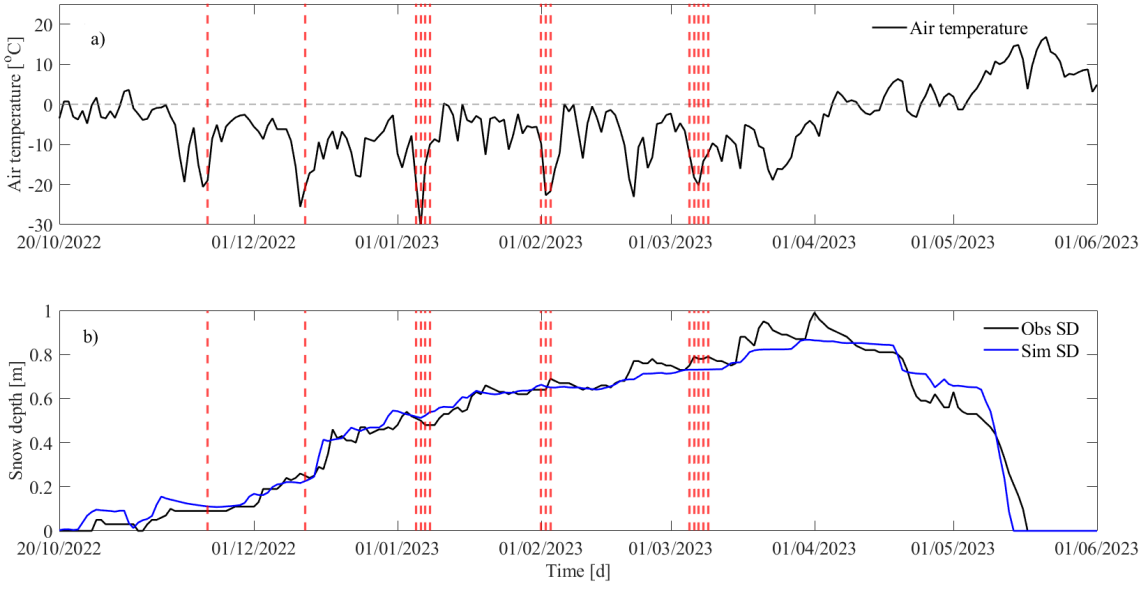

Figure 5. a) Observed air temperature and b) observed (Obs SD) and simulated (Sim SD) snow depths. Red vertical lines are frost quakes observed by Afonin et al. (2024). Grey horizontal line (a) shows 0 C degree.

https://doi.org/10.5194/egusphere-2026-2611
Preprint. Discussion started: 30 June 2026

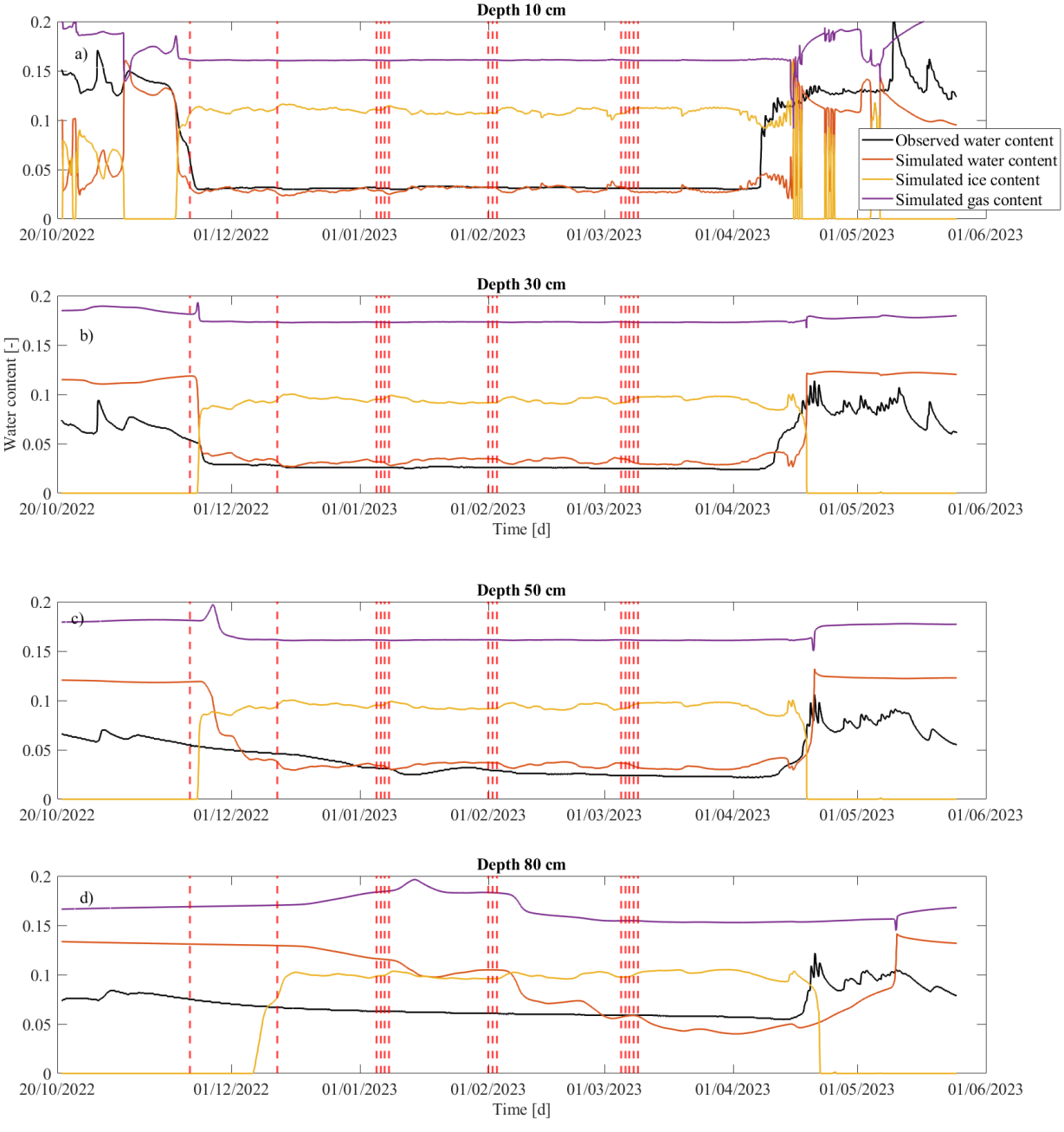

Figure 6. Dimensionless volume fractions water, ice and gas contents of soil at the depths of 10 cm, 30 cm, 50 cm, and 80 cm during the period 20.10.2022–29.6.2023. Red vertical lines are observed frost quakes.

https://doi.org/10.5194/egusphere-2026-2611
Preprint. Discussion started: 30 June 2026

Figure 6 presents the simulated gas (air), water, and ice content at depths of 10 cm, 30 cm, 50 cm, and 80 cm. ATS simulations confirm that air is always present in the soil, with air content varying between 0.09–0.21 (10 cm), 0.015–0.19 (30 cm), 0.15–0.20 (50 cm), and 0.15–0.20 (80 cm). Maximum air content was reached in late November to early December as freezing began, while the lowest values occurred during the freezing period from early December to mid-May.

During the freezing period, simulated and observed water content aligned at depths of 10 cm, 30 cm, and 50 cm, but at 80 cm the observed water content was higher than simulated. There are slight variations in the simulated water contents at the depths of 10 cm and 30 cm, which coincide with observed and simulated soil temperatures (Figure 7 a, b). In April–May, when the soil remained frozen, the sudden increase in observed water content at all depths was not reflected in the simulations. This discrepancy may be due to the soil probes registering slight water content increases even at subzero temperatures. While ice content remained relatively stable during freezing, slight increases when water content decreases coincided with frost quakes (Figure 6 and Figure 8d). This pattern was observed at all depths, including at 80 cm.

Figure 7 compares soil temperatures obtained from observation and ATS simulation. Soil temperature followed air temperature trends, with the variation of the amplitude in temperature being greatest at the depth of 10 cm and smallest at 80 cm. Observations indicate that the soil remained frozen during the period 17.11.2023–8.5.2023 (173 days), 22.11.2023–10.5.2024 (170 days), 17.12.2023–13.5.2024 (148 days), 27.3.2024–23.4.2024 (28 days), at the depths of 10 cm, 30 cm, 50 cm, and 80 cm, respectively. Simulated onset of freezing was the same earlier and lasted a little less than observed. Simulated and observed temperatures show similar dynamics, except between mid-April and mid-May when the snow melts. The simulated temperature reacts to air temperature variations but CS615 temperature probes did not (cf. Section 2). During freezing period (except from mid-April to mid-May) the simulated minimum temperature can be up to 1 °C colder than the observed soil temperature.

3.2 Cryosuction simulation and observed frost quakes

Figure 8 shows the air temperature, simulated profiles of soil temperature, cryosuction, soil water and ice content from ATS. When air temperature dropped – often coinciding with frost quakes occurrence – soil temperature and water content decrease and soil ice content and cryosuction increase. It is worth noting that there are a few instances of capillary pressure increase but frost quakes are masked by the ice quakes in river Kitinen Afonin et al. (2024).

https://doi.org/10.5194/egusphere-2026-2611
Preprint. Discussion started: 30 June 2026

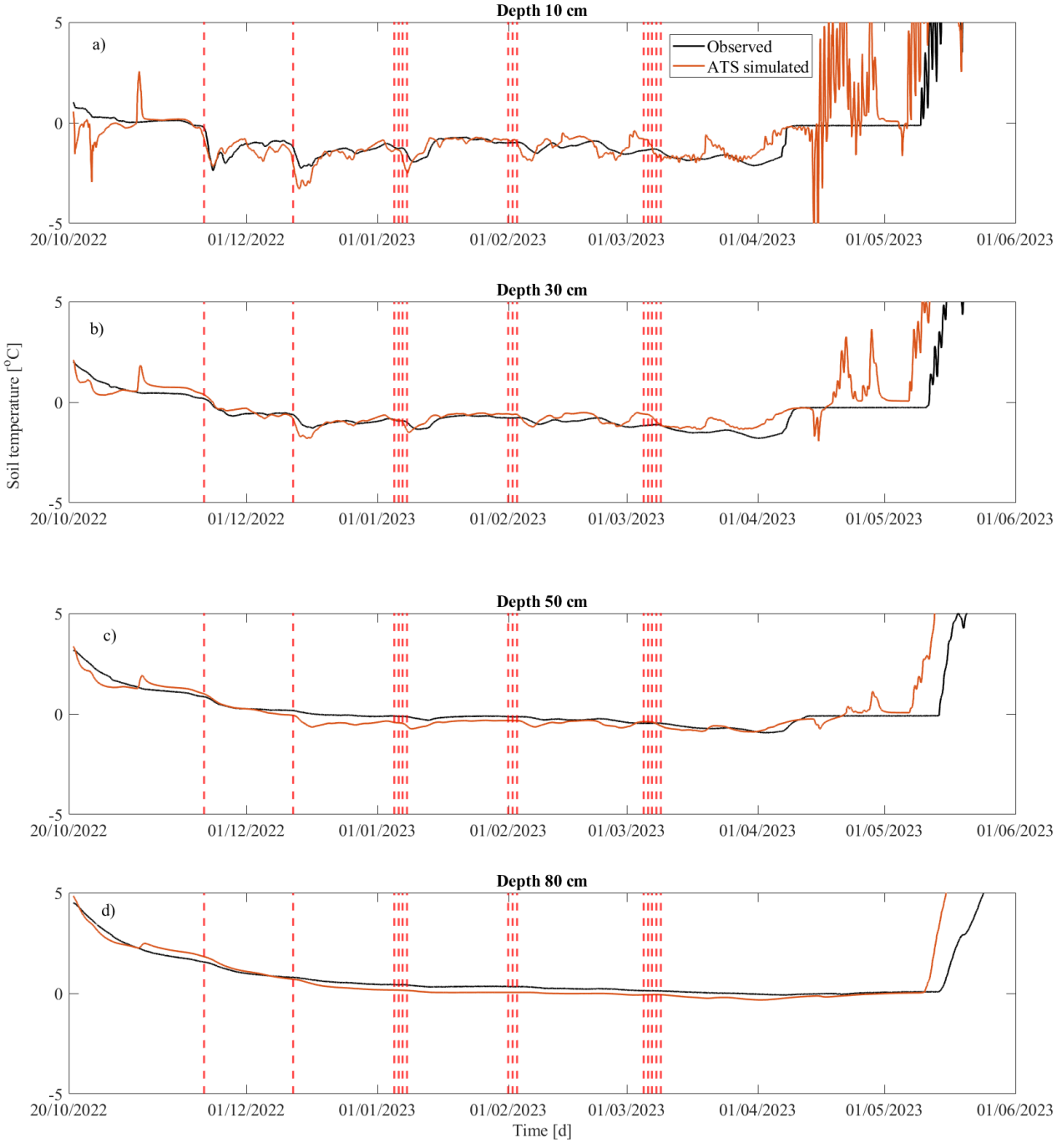

Figure 7. Simulated and observed soil temperatures at depths (a) 10 cm, (b) 30 cm, (c) 50 cm and (d) 80 cm depths during the period 20.10.2022 – 29.6.2023. Red vertical lines are observed frost quakes.

https://doi.org/10.5194/egusphere-2026-2611
Preprint. Discussion started: 30 June 2026

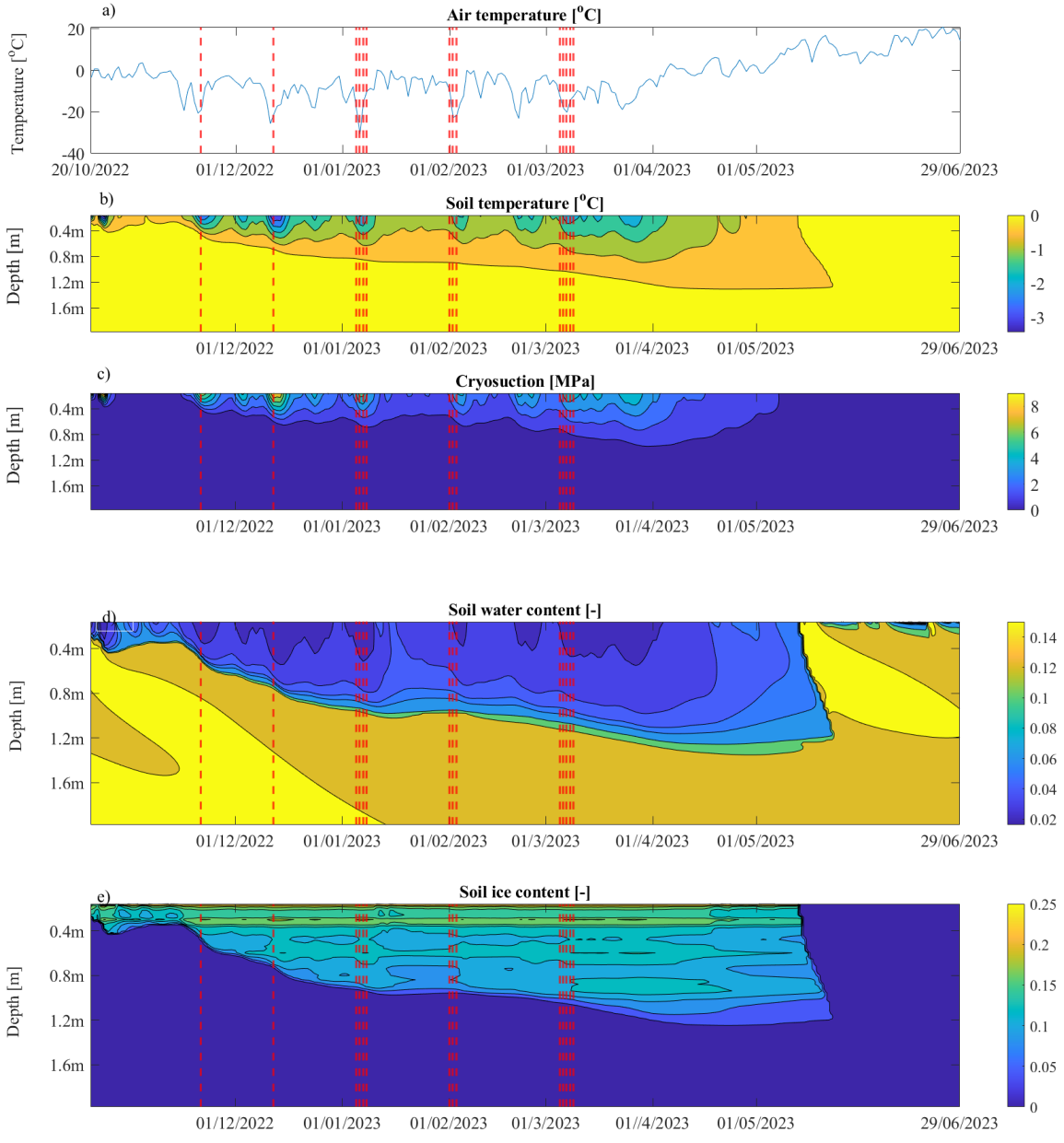

Figure 8. a) Observed air temperature, ATS simulation results for b) soil temperature, c) cryosuction, d) soil water content, e) soil ice content during the period 20.10.2022 – 29.6.2023. Red vertical lines are frost quakes observed by Afonin et al. (2024).

.

https://doi.org/10.5194/egusphere-2026-2611
Preprint. Discussion started: 30 June 2026

4 Results of thermo-mechanical analysis

Here we present the OGS simulation results. From the full time series we only evaluate the last season, where the frost quake event data is available. The indicator function (7) is chosen such that the phase transition starts at T_m and is completed at $-2°\mathrm{C}$ (i. e. $S_\mathrm{I} \approx 0.99$). This way, more realistic soil freezing characteristics are achieved. Below-zero temperatures quickly convert all pore water into ice, as shown in Figure 9b.

(a) Lateral stress rate as a function of temperature rate.
(Note the linear scale in the middle section of each axis and the logarithmic one outside.)

(b) Ice saturation as a function of temperature.

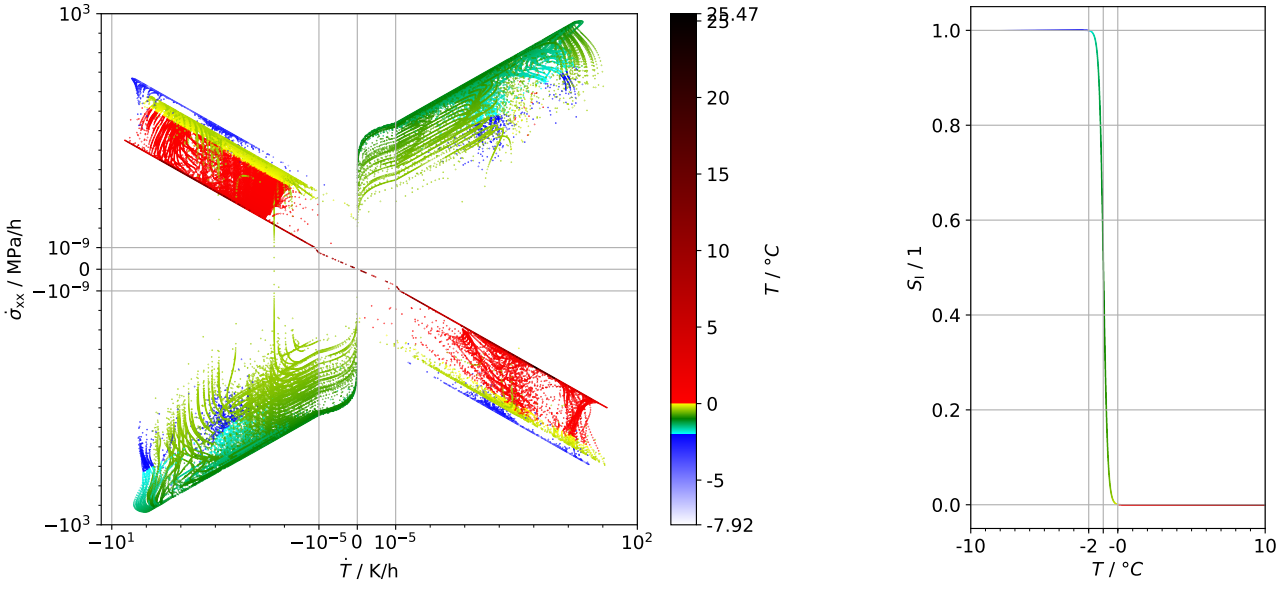

Figure 9. Influence of temperature changes on lateral stress rates (assuming $\varepsilon_{xx} = 0$) and effect of temperature on ice saturation.

Figure 9a illustrates the effect of temperature rates $\dot{T}$ on the lateral stress rate $\dot{\sigma}_{xx}$ across all model integration points and all times. Basically, we can divide the diagram into four quadrants with respect to the sign of $\dot{T}$ and $\dot{\sigma}_{xx}$. There is and obvious red line for unfrozen soil from the top left to the bottom right quadrant. This red line indicates lateral unloading (i. e. a tendency towards tension) during cooling and lateral compression during heating, caused by the soil's thermal expansion. Similarly, the blue points mostly show higher stress rates in frozen soil due to the ice's greater thermal expansion coefficient. Points in the top right and bottom left quadrants undergo phase transitions with cooling leading to compression and heating relieving it, which is linked to the constrained volumetric expansion of ice formation. The vertical spread in these clusters is related to the nonlinearity introduced in the thermal and mechanical properties by the phase-transition function (7).

The depth-dependent state is plotted for several seasonal cycles in Figure 10. While atmospheric temperature changes have significant consequences until around 2 m depth (Fig. 10b), ice formation occurs up to 1 m depth (Fig. 10c). Frost heave is

https://doi.org/10.5194/egusphere-2026-2611
Preprint. Discussion started: 30 June 2026

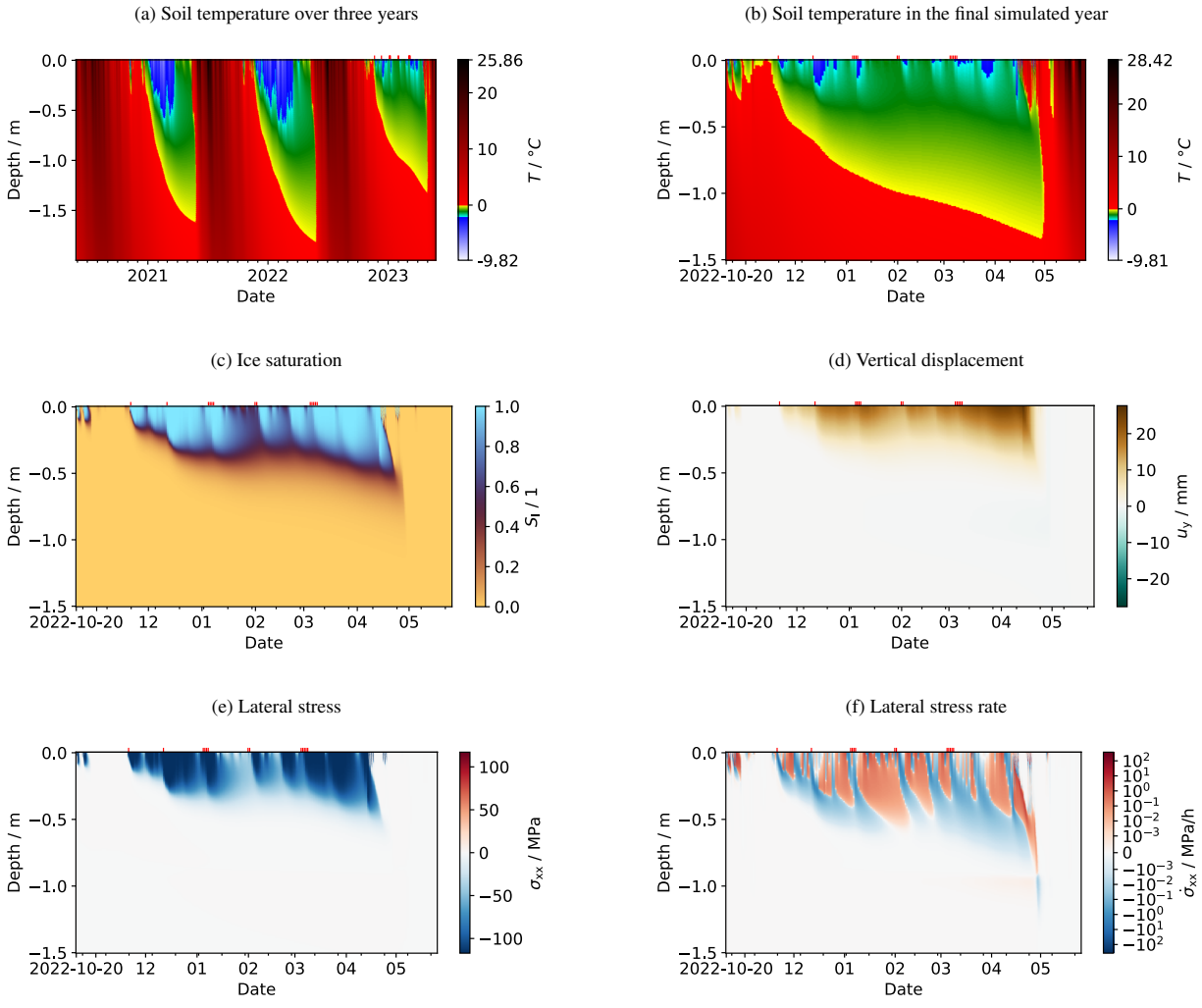

Figure 10. Temporal development of key quantities from OGS simulations over the depth. Red marks on the upper horizontal axis indicate seismic events observed by Afonin et al. (2024).

associated with freezing (Fig. 10d) and lateral stress changes occur in the frozen region (Fig. 10f). We can see that the highest compressive stress rates (blue) occur at the freezing front where the expansion of the ice body is constrained. The same is true for the melting front, where we see the strongest lateral unloading. In the frozen soil body, tensile stress rates associated with thermal contraction become visible at several instances indicated by paler red tones. Interestingly, these extend through larger parts of the ice body simultaneously rather than exhibiting a frontal character, as the heat diffusion is not hindered by latent heat effects in this case. Explanations for these phenomena are in line with those given for Figure 9a.

https://doi.org/10.5194/egusphere-2026-2611
Preprint. Discussion started: 30 June 2026

As the stress state is not isotropic and there is a principal stress difference ($\sigma_1 = \sigma_{xx}, \sigma_2 = \sigma_{yy} \approx 0$), shear stresses must be present in the simulated soil:

$$\tau = |\sigma_{\max}| = |\sigma_1 - \sigma_2|/2 = |\sigma_{xx} - \sigma_{yy}|/2 \approx |\sigma_{xx}/2| \tag{10}$$

Hence, the distribution of the shear stress equals the one of the lateral stress (Fig. 10e).[7] In Figure 10e a highly compressed and sheared soil horizon with varying depth is clearly visible. Looking on the stress rates in Figure 10f, a sharp border becomes visible: The white line marks the moving boundary between highly compressive and highly tensional stress rates. Note that there is a specific depth of this moving boundary, changing with time. This way, material points can change rapidly from compressive to tensional stress rates.

It is clear that the formation and expansion of ice and subsequent thermal straining of the frozen soil can build up significant potential energy. As for the energy release during frost quakes, the simulation results suggest three mechanisms:

1. tensional lateral stress rates being critical for geomaterials (crack opening mode I),
2. compressive lateral stress rates leading to buckling instabilities,[8]
3. shear stresses leading to shear failure (crack opening mode II, III, or mixed).

5 Discussion

In this study, we presented both seismological observations as well as two distinct modeling approaches to investigate the underlying mechanisms behind frost quakes.

In previous studies (e. g. Battaglia and Changnon, 2016; Okkonen et al., 2020) frost quakes were associated with little or no snow, snow melt or rainfalls prior to sudden decline of air temperature. Soil undergoes fast freezing and cracks are supposed to be due to the expansion of freezing water. Afonin et al. (2024) found that frost quakes can occur during thick snow cover and no prior melting/rainfalls. In this study, we show that frost quakes occurred during conditions when soil was covered by snow, top soil was frozen, soil temperature decreased and cryosuction increased.

Different studies (e. g. Style et al., 2011; Gerber et al., 2022, 2023; Style et al., 2023) have shown freezing induced stresses by cryosuction. Gerber et al. (2022, 2023) showed that grooves can transport water towards regions with colder temperatures and large stresses can build up directly adjacent to the grooves and eventually break materials. In confining materials, such as soils, the stress distribution defines how soils will crack. In frost quakes, vertical cracks extend through the ice body and the thicker the ice body, the larger the frost quakes and damage potential (Okkonen et al., 2020; Afonin et al., 2024).

It is known that below freezing temperature, water can be sucked into pore space causing ice to grow, pushing open the pore, building-up pressure and damaging the material. We observed that frost quakes occurred when cryosuction pressure increased and air temperature fell below -20 °C (cf. Figs. 5 and 8), except on 21.2.2023, when ice quake events in the nearby Kitinen

[7] Note that lateral stresses should remain unspecific: due to the strict BCs absolute values might be too high.
[8] This cannot happen in the idealized simulations, but only in a real geological setting.

https://doi.org/10.5194/egusphere-2026-2611
Preprint. Discussion started: 30 June 2026

River masked soil frost quakes (Afonin et al., 2024). The increase in cryosuction pressure and ice content in combination with a decrease in air and soil temperatures and water content (cf. Fig. 8) aligns with predictions from the Clapeyron equation (Eq. 3) and thermal stress calculations by Okkonen et al. (2020). However, we cannot conclusively state, based on the 1D thermo-hydrological simulations, that sudden energy release was a direct consequence of increase in cryosuction pressure, water flow into pore space, ice accumulation and stress buildup.

The thermo-mechanical simulations with OGS showed that both horizontal and vertical stresses build upon freezing. Vertical stress is relieved by frost heave (uplift of soil). Lateral stresses are compressive (blue color in Fig. 10e) and seem to associate with frost quake events. However, the simulations cannot support the hypothesis that frost heave causes tension at the soil surface bending the frozen soil body upward (uplift) and potentially causing vertical cracks. On the other hand, the simulated stress *rate* changes rapidly both temporally and spatially (vertically), which may also lead to cracking. Moreover, in reality, cold spell could cause shrinkage and high tensile stress rates to develop.

From the simplifying simulation assumptions it is clear that the overall physical process could only be captured by parts. In particular, a plastic reaction of the soil matrix due to ice expansion must be assumed. However, this is considered as a post-critical state in this study.

Note that both for ATS and OGS simulations, the temperature rates imposed to the top boundary as well as the results calculated from that depend largely on the sampling rate at which the temperature signal is given. The coarser this time step in the temperature signal, the lower the rates. Fast temperature changes will mostly act superficially, though, as the thermal capacity of the soil causes damping. From a length-scale of interest, one could deduce a corresponding time scale and hence a proper sampling rate.

Our analysis of snow depth and moisture conditions of the soil at the time of frost quakes as well as potential fracturing mechanisms inferred from the thermo-mechanical simulations challenge conventional explanations for the phenomenon, such as those summarized by Battaglia and Changnon (2016). To be precise, our results challenge the prevalent assumptions about both the meteorological conditions behind frost quake occurrence and that the phenomenon would be driven by cryosuction effects, stress buildup at the top, within and at the bottom of the frozen soil body.

Overall, our results suggest that a more complete thermo-hydro-mechanical modeling (Norouzi and Li, 2024) is needed to fully understand the processes and conditions behind frost quakes, especially since compression- and contraction-driven stress accumulation may play a more significant role in frost quake initiation than previously assumed. Experimental validation remains crucial. While Zoet et al. (2020) successfully induced ice quakes in a controlled setting, similar studies on frost quakes are lacking. Since different mechanisms likely scale differently with cooling rates and temperature conditions, controlled experiments could help to distinguish between contraction-driven and expansion-driven processes including the role of cryosuction. Our findings call for a reassessment of commonly accepted frost quake formation mechanisms and highlight the need for further studies to improve predictive models in cold climate regions.

https://doi.org/10.5194/egusphere-2026-2611
Preprint. Discussion started: 30 June 2026

6 Conclusions

This study challenges the conventional understanding of frost quake occurrence by demonstrating that frost quake events can occur under conditions not previously emphasized, including thick snow cover and without prior melt or rainfall. Our thermo-hydrological simulations show that cryosuction, ice accumulation, and temperature decline coincide with frost quake event, the results do not provide conclusive evidence that these processes alone directly trigger frost quakes. Instead, our thermo-mechanical simulations indicate that both compressive and contraction driven stresses, particularly lateral stresses, may play a more significant role. Our findings highlight limitations in current modeling approaches, which capture only parts of the complex thermo-hydro-mechanical interactions. Consequently, a more comprehensive modeling framework, combined with controlled experimental validation, is necessary to better understand the mechanisms driving frost quakes. Overall, this work calls for a reassessment of existing modeling frameworks and underscores the need for fully integrated thermo-hydro-mechanical models and further research to improve prediction and risk assessment in cold region environments.

Code and data availability. Thermo-hydrological simulations were conducted using the Advanced Terrestrial Simulator (ATS) version 1.3 (Coon et al., 2022, https://doi.org/10.5281/zenodo.6679807), available at https: //github.com/amanzi/ats. Thermo-Mechanical simulations were conducted using OpenGeoSys. Kolditz et al. 2012, available at https://gitlab.opengeosys.org/ogs/ogs. climate forcing data source for the site are from https://www.ilmatieteenlaitos.fi/havaintojen-lataus,

Appendix A: Material parameters

Parameter	symbol/unit	S	I	W
thermal conductivity	$\lambda_{\mathrm{XR}}/\mathrm{W\,m^{-1}\,K^{-1}}$	2.69	2.2	0.58
specific heat capacity	$c_{p\mathrm{X}}/\mathrm{J\,kg^{-1}\,K^{-1}}$	840	2095	4190
mass density	$\rho_{\mathrm{XR}}/\mathrm{kg\,m^{-3}}$	2625	910	1000
thermal expansivity	α_T^{X} / $\mathrm{K^{-1}}$	10^{-6}	$5.17 \cdot 10^{-5}$	0
Young's modulus	E_{X} / Pa	$53 \cdot 10^6$	$9.0 \cdot 10^9$	–
Poisson's ratio	ν_{X} / 1	0.3	0.32	–

Table A1. Material parameters for the phases $\mathrm{X} \in \{\mathrm{S, W, I}\}$, i. e. solid (S), water (W) and ice (I)

Author contributions. Jarkko Okkonen: Conceptualization, Thermal-Hydrological simulation, writing original draft Christian B. Silbermann: Conceptualization, Writing - review and editing. Dmitri Naumov: Conceptualization, Thermal-Mechanical simulations, Writing - review and editing. Jere Remes: Conceptualization, Methodology, Thermal-Mechanical simulations, writing Nikita Afonin: Seismic recordings and data analysis, Writing. Elena Kozlovskaya: Resources, Seismic recordings and data analysis, Writing - review and editing. Emma-

https://doi.org/10.5194/egusphere-2026-2611
Preprint. Discussion started: 30 June 2026

Riikka Kokko: Collecting and analyzing soil data. Kari Moisio: Seismic recordings, Writing -review and editing. Tymofiy Gerasimov: Conceptualization, Writing - review and editing. Thomas Nagel: Conceptualization, Supervision, Writing - review and editing.

Competing interests. The authors declare no competing interests.

Acknowledgements. This study is a part of the ADAPTINFA (Urban Environment and Climate Change in the Arctic: Data-driven Intelligence Approach to Multihazard Mitigation) project funded by the Research Council of Finland in 2022–2024 and CRYO-RI (Cryosphere Research Infrastructure Platform) project funded by the Research Council of Finland in 2023–2025. Ethan Coon and Scott Painter are thanked for insightful conversations on the topic as well as their hospitality during the research visit to Oak Ridge National Laboratory, USA.

Financial support. This research has been supported by the Research Council of Finland (grant no. 348802, 348811, 352759)

https://doi.org/10.5194/egusphere-2026-2611
Preprint. Discussion started: 30 June 2026

References

Afonin, N. and Kozlovskaya, E.: Development of events detector for monitoring cryoseisms in upper soils., XXIX Geofysiikan päivät : Rovaniemellä 21.-22.3.2019, pp. 13–15, https://urn.fi/URN:NBN:fi-fe202003208608, 2019.

Afonin, N., Kozlovskaya, E., Moisio, K., Kokko, E.-R., and Okkonen, J.: Frost quakes in wetlands in northern Finland during extreme winter weather conditions and related hazard to urban infrastructure, The Cryosphere, 18, 2223–2238, https://doi.org/10.5194/tc-18-2223-2024, 2024.

Arola, T., Okkonen, J., and Jokisalo, J.: Groundwater utilisation for energy production in the Nordic environment: An energy simulation and hydrogeological modelling approach, Journal of Water Resource and Protection, 8, 642–656, https://doi.org/10.4236/jwarp.2016.86053, 2016.

Aukenthaler, M., Brinkgreve, R. B., and Haxaire, A.: Evaluation and application of a constitutive model for frozen and unfrozen soil, Proceedings of the GeoVancouver: the 69th Canadian Geotechnical Conference, Vancouver, Canada (pp. 1-8), pp. 1–8, 2016.

Battaglia, S. M. and Changnon, D.: Frost quakes: Forecasting the unanticipated clatter, Weatherwise, 69, 20–27, https://doi.org/10.1080/00431672.2015.1109984, 2016.

Bilke, L., Flemisch, B., Kalbacher, T., Kolditz, O., Helmig, R., and Nagel, T.: Development of open-source porous media simulators: principles and experiences, Transport in porous media, 130, 337–361, https://doi.org/10.1007/s11242-019-01310-1, 2019.

Bluhm, J., Ricken, T., and Bloßfeld, M.: Ice formation in porous media, in: Advances in Extended and Multifield Theories for Continua. Lecture Notes in Applied and Computational Mechanics, edited by Markert, B., pp. 173–174, Springer, Berlin, https://doi.org/https://doi.org/10.1007/978-3-642-22738-7_8, 2011.

Brantley, S. L., Goldhaber, M. B., and Ragnarsdottir, K. V.: Crossing disciplines and scales to understand the critical zone, Elements, 3, 307–314, https://doi.org/https://doi.org/10.2113/gselements.3.5.307, 2007.

Coon, E. T., Moulton, J. D., Kikinzon, E., Berndt, M., Manzini, G., Garimella, R., Lipnikov, K., and Painter, S. L.: Coupling surface flow and subsurface flow in complex soil structures using mimetic finite differences, Advances in Water Resources, 144, 103 701, https://doi.org/https://doi.org/10.1016/j.advwatres.2020.103701, 2020.

Derjaguin, B. and Churaev, N.: The theory of frost heaving, Journal of Colloid and Interface Science, 67, 391–396, https://doi.org/https://doi.org/10.1016/0021-9797(78)90227-8, 1978.

Evans, R. and Untersteiner, N.: Thermal cracks in floating ice sheets, Journal of Geophysical Research, 76, 694–703, https://doi.org/https://doi.org/10.1029/JC076i003p00694, 1971.

Finnish Meterorological Institute Open Data, Weather Observations: Open data services. Helsinki, Finland: Finnish Meteorological Institute, https://www.ilmatieteenlaitos.fi/havaintojen-lataus, Accessed:20.08.2024.

Gao, B. and Coon, E. T.: Evaluating simplifications of subsurface process representations for field-scale permafrost hydrology models, The Cryosphere, 16, 4141–4162, https://doi.org/10.5194/tc-16-4141-2022, 2022.

Gerber, D., Wilen, L. A., Poydenot, F., Dufresne, E. R., and Style, R. W.: Stress accumulation by confined ice in a temperature gradient, Proceedings of the National Academy of Sciences, 119, e2200748 119, https://doi.org/10.1073/pnas.2200748119, 2022.

Gerber, D., Wilen, L. A., Dufresne, E. R., and Style, R. W.: Polycrystallinity Enhances Stress Buildup around Ice, Physical Review Letters, 131, 208 201, https://doi.org/https://doi.org/10.1103/PhysRevLett.131.208201, 2023.

Giardino, J. R. and Houser, C.: Principles and dynamics of the critical zone, Elsevier, https://shop.elsevier.com/books/principles-and-dynamics-of-the-critical-zone/giardino/978-0-444-63369-9, 2015.

https://doi.org/10.5194/egusphere-2026-2611
Preprint. Discussion started: 30 June 2026

Gilpin, R. R.: A model for the prediction of ice lensing and frost heave in soils, Water Resources Research, 16, 918–930, https://doi.org/https://doi.org/10.1029/WR016i005p00918, 1980.

Goto, K., Hamaguchi, H., and Wada, Y.: A study on ice faulting and icequake activity in the Lake Suwa.(3) Icequake activity and thermal stresses in ice plate, Ph.D. thesis, Tohoku University, https://www.google.com/url?sa=t&source=web&rct=j&opi=89978449&url=https://tohoku.repo.nii.ac.jp/record/11764/files/AA0045942680788.pdf&ved=2ahUKEwiJwZ-irPyUAxVuHxAIHUq8MhAQFnoECBkQAQusg=AOvVaw1JW-SO1Q_2NQIMcEAw3cyO, 1980.

Haxaire, A., Aukenthaler, M., and Brinkgreve, R.: Application of a thermo-hydro-mechanical model for freezing and thawing, in: ISRM European Rock Mechanics Symposium EUROCK 2017, pp. 74–81, ISRM, ISSN 1877-7058, https://doi.org/https://doi.org/10.1016/j.proeng.2017.05.156, 2017.

IPCC: Climate Change 2023: Synthesis Report. Contribution of Working Groups I, II and III to the Sixth Assessment Report of the Intergovernmental Panel on Climate Change, IPCC, Geneva, Switzerland, 131, 35–115, 2023.

Kavanaugh, J., Schultz, R., Andriashek, L. D., van der Baan, M., Ghofrani, H., Atkinson, G., and Utting, D. J.: A New Year's Day icebreaker: icequakes on lakes in Alberta, Canada, Canadian Journal of Earth Sciences, 56, 183–200, https://doi.org/10.1139/cjes-2018-0196, 2019.

Kolditz, O., Bauer, S., Bilke, L., Böttcher, N., Delfs, J. O., Fischer, T., Görke, U. J., Kalbacher, T., Kosakowski, G., McDermott, C. I., Park, C. H., Radu, F., Rink, K., Shao, H., Shao, H. B., Sun, F., Sun, Y. Y., Singh, A. K., Taron, J., Walther, M., Wang, W., Watanabe, N., Wu, Y., Xie, M., Xu, W., and Zehner, B.: OpenGeoSys: an open-source initiative for numerical simulation of thermo-hydro-mechanical/chemical (THM/C) processes in porous media, Environmental Earth Sciences, 67, 589–599, https://doi.org/10.1007/s12665-012-1546-x, 2012.

Korshunov, A. A., Churkin, S. V., and Nevzorov, A. L.: Calibration of PLAXIS frozen/unfrozen soil model according to results of laboratory tests and in-situ monitoring, in: Transportation Soil Engineering in Cold Regions, Volume 2: Proceedings of TRANSOILCOLD 2019, pp. 105–120, Springer, ISBN 978-981-15-0453-2, https://doi.org/10.1007/978-981-15-0454-9_12, 2020.

Laine, L.: Frost quake caused crack in house in Talvikangas—A massive boom was heard from kilometers, Kaleva, 15.1.2016, https://www.kaleva.fi/jaajaristys-halkaisi-talon-talvikankaalla-valtava/1781214, 2016.

Leung, A. C. W., Gough, W. A., and Shi, Y.: Identifying frostquakes in Central Canada and neighbouring Regions in the United States with Social Media, in: Citizen empowered mapping, Geotechnologies and the Environment (Vol. 18, pp. 1–26), edited by Leitner, M. and Jokar Arsanjani, J., Springer, https://doi.org/https://doi.org/10.1007/978-3-319-51629-5_9, 2017.

Lombardi, D., Gorodetskaya, I., Barruol, G., and Camelbeeck, T.: Thermally induced icequakes detected on blue ice areas of the East Antarctic ice sheet, Annals of Glaciology, 60, 45–56, https://doi.org/10.1017/aog.2019.26, 2019.

Marttila, H., Aurela, M., Büngener, L., Rossi, P., Lohila, A., Postila, H., Saari, M., Penttilä, T., and Kløve, B.: Quantifying groundwater fluxes from an aapa mire to a riverside esker formation, Hydrology Research, 52, 585–596, https://doi.org/https://doi.org/10.2166/nh.2021.064, 2021.

Naumov, D., Bilke, L., Lehmann, C., Fischer, T., Wang, W., Shao, H., Buchwald, J., Rink, K., Chen, C., Mollaali, M., Kessler, K., and Max, J.: OpenGeoSys, https://doi.org/10.5281/zenodo.13685289, 2024.

Norouzi, E. and Li, B.: Finite element modeling of thermal-hydro-mechanical coupled processes in unsaturated freezing soils considering air-water capillary pressure and cryosuction, International Journal for Numerical and Analytical Methods in Geomechanics, 48, 2944–2970, https://doi.org/10.1002/nag.3761, 2024.

Odong, J.: Evaluation of empirical formulae for determination of hydraulic conductivity based on grain-size analysis, Journal of American Science, 3, 54–60, 2007.

https://doi.org/10.5194/egusphere-2026-2611
Preprint. Discussion started: 30 June 2026

Okkonen, J., Neupauer, R., Kozlovskaya, E., Afonin, N., Moisio, K., Taewook, K., and Muurinen, E.: Frost quakes: Crack formation by thermal stress, Journal of Geophysical Research: Earth Surface, 125, e2020JF005 616, https://doi.org/https://doi.org/10.1029/2020JF005616, 2020.

Painter, S. L. and Karra, S.: Constitutive model for unfrozen water content in subfreezing unsaturated soils, Vadose Zone Journal, 13, 1–8, https://doi.org/https://doi.org/10.2136/vzj2013.04.0071, 2014.

Parsekian, A., Singha, K., Minsley, B. J., Holbrook, W. S., and Slater, L.: Multiscale geophysical imaging of the critical zone, Reviews of Geophysics, 53, 1–26, https://doi.org/https://doi.org/10.1002/2014RG000465, 2015.

Peppin, S. S. L. and Style, R. W.: The physics of frost heave and ice-lens growth, Vadose Zone Journal, 12, vzj2012.0049, https://doi.org/https://doi.org/10.2136/vzj2012.0049, 2013.

Rantanen, M., Karpechko, A. Y., Lipponen, A., Nordling, K., Hyvärinen, O., Ruosteenoja, K., Vihma, T., and Laaksonen, A.: The Arctic has warmed nearly four times faster than the globe since 1979, Communications earth & environment, 3, 168, https://doi.org/https://doi.org/10.1038/s43247-022-00498-3, 2022.

Schollick, S., Curran, W., Dufresne, W., Velikov, D., and Aarts: Segregated Ice Growth in a Suspension of Colloidal Particles, J Phys Chem B., https://doi.org/doi: 10.1021/acs.jpcb.6b00742, 2016.

Schweitzer, J., Fyen, J., Mykkeltveit, S., Gibbons, S. J., Pirli, M., Kühn, D., and Kværna, T.: Seismic arrays, in: New manual of seismological observatory practice 2 (NMSOP-2), pp. 1–80, Deutsches GeoForschungsZentrum GFZ, 2012.

Sipola, T.: Jokisen perheen talo halkesi kahdeksan vuotta sitten – nyt samaa ilmiötä ihmetellään Chicagossa, YLE, 13.2.2024, https://yle.fi/a/74-20073680, 2024.

Sjöberg, Y., Coon, E., K. Sannel, A. B., Pannetier, R., Harp, D., Frampton, A., Painter, S. L., and Lyon, S. W.: Thermal effects of groundwater flow through subarctic fens: A case study based on field observations and numerical modeling, Water Resources Research, 52, 1591–1606, https://doi.org/https://doi.org/10.1002/2015WR017571, 2016.

Style, R. W., Peppin, S. S. L., Cocks, A. C. F., and Wettlaufer, J. S.: Ice-lens formation and geometrical supercooling in soils and other colloidal materials, Phys. Rev. E, 84, 041 402, https://doi.org/10.1103/PhysRevE.84.041402, 2011.

Style, R. W., Gerber, D., Rempel, A. W., and Dufresne, E. R.: The generalized Clapeyron equation and its application to confined ice growth, Journal of Glaciology, 69, 1091–1096, https://doi.org/10.1017/jog.2023.28, 2023.

Tuohino, M., Solowski, W., Abed, A., Koivisto, K., and Lei, X.: Application of the Frozen and Unfrozen Soil model to modelling effects of freeze-thaw on low-volume roads, in: IOP Conference Series: Earth and Environmental Science, vol. 710, p. 012067, IOP Publishing, https://doi.org/10.1088/1755-1315/710/1/012067, 2021.

van Genuchten, M. T.: A closed-form equation for predicting the hydraulic conductivity of unsaturated soils, Soil science society of America journal, 44, 892–898, https://doi.org/https://doi.org/10.2136/sssaj1980.03615995004400050002x, 1980.

Zheng, T., Miao, X.-Y., Shao, H., Kolditz, O., Nagel, T., and Naumov, D.: A thermo-hydro-mechanical finite element model of freezing in porous media-thermo-mechanically consistent formulation and application to ground source heat pumps, in: COUPLED VII: proceedings of the VII International Conference on Computational Methods for Coupled Problems in Science and Engineering, pp. 1008–1019, CIMNE, http://hdl.handle.net/2117/190800, 2017.

Zheng, T., Miao, X.-Y., Naumov, D., Shao, H., Kolditz, O., and Nagel, T.: A thermo-hydro-mechanical finite-element model with freezing processes in saturated soils, Environmental Geotechnics, 9, 502–514, https://doi.org/10.1680/jenge.18.00092, 2022.

Zoet, L., Ikari, M., Alley, R. B., Marone, C., Anandakrishnan, S., Carpenter, B., and Scuderi, M. M.: Application of constitutive friction laws to glacier seismicity, Geophysical Research Letters, 47, e2020GL088 964, https://doi.org/https://doi.org/10.1029/2020GL088964, 2020.